Self-assembly of defect-free nanostripe arrays on B-doped Si(001)

Ivan Ermanoski, Norman C. Bartelt, and Garry L. Kellogg

Phys. Rev. B **83**, 205432 — Published 31 May 2011

DOI: 10.1103/PhysRevB.83.205432

Self-assembly of defect-free nano-stripe arrays on B-doped Si(001)

Ivan Ermanoski*, Norman C. Bartelt and Garry L. Kellogg

Sandia National Laboratories, Albuquerque, New Mexico, 87185-1415, USA

and Sandia National Laboratories, Livermore, California 94551, USA

Received: 28.03.2011

ABSTRACT We have developed a method to grow large, self-assembled, defect-free arrays of vacancy or adatom stripes on atomically flat, boron-doped Si(001)-(2x1). The sub-nanometer-high stripes form between ~870°C and 990°C, with a spacing that depends on temperature. Si deposition is used to prevent sublimation-induced defect formation and to allow time for ordering via surface diffusion. Ordering mechanisms, observed in real time by low energy electron microscopy (LEEM), include island nucleation and growth, longitudinal splitting, and coarsening. At formation temperatures, the arrays are only stable when the area fractions of vacancy (θ_v) or adatom stripes (θ_a) are ~½, consistent with stress domain theory predictions. At room temperature, arrays are preserved indefinitely and are a potential template for nanowire growth.

PACS: 68.35.bg, 64.75.Yz, 68.37.Nq, 68.35.Md

* corresponding author: iermano@sandia.gov

Self-assembled surface nanostructures have the potential to allow structural, chemical, or electrical properties to be tailored for particular technological applications. Thus, considerable theoretical and experimental effort has been devoted to understanding how they form.[1] Ideally, one wishes to produce many uniform structures with a minimum number of defects. Relatively little effort, however, has been focused on understanding how various defects form, and how they can be removed. In this paper we report a method to produce defect-free self-assembled structures on the technologically important Si(001)-(2x1) surface.

Striped patterns form spontaneously on B-doped Si(001) surfaces[2] and are an appealing substrate for templated adsorbate deposition or nanowire growth. Self-assembly of this nature has been interpreted in terms of relaxation of surface stress.[3-8] Stripe boundaries consist of long S_A atomic steps (where the upper terrace dimer rows of the Si(001)-(2x1) reconstruction are parallel to the step) and much shorter (perpendicular) S_B steps. Stripe morphology depends on sample temperature, explained by Hannon et al. in terms of a temperature dependent, boron-induced lowering of the S_A free energy per unit length (β_A).[9, 10] The role of boron in the stripe formation process has been studied in detail on the atomic level[11, 12] to some extent, but the precise mechanism of action remains unclear.

Even on nominally flat Si surfaces, naturally-occurring steps limit stripe lengths. For example, the terrace width (defined by $w=h/\tan\alpha$, where w is the step separation, h is the step height, and α is the angle of miscut) is only 78 nm for $\alpha=0.1°$. To overcome this limitation, Tanaka et al. proposed a method of creating large step-free regions on Si(001) via etching an array of pits onto the surface, and heating to high temperature in ultrahigh vacuum (UHV).[13] This causes the formation and successive expansion of oval vacancy islands at pit bottoms, eventually creating large step-free terraces. Nielsen et al. used such patterned surfaces to create extended stripe arrays by Si and B_2H_6 co-deposition.[14] These stripe arrays are considerably larger (~10 μm a side, with tens of stripes) than on non-patterned substrates (<0.1 μm), but still include defects such as randomly positioned and incompletely formed (fork-shaped) stripes. Herein we discuss the role of sublimation in the formation of these and other defects, and show that they can be avoided or removed at high temperature by depositing Si during self-assembly. We also show

that defect-free arrays are well-suited for comparison with stress-domain theory predictions, such as stripe spacing dependence on temperature, and equilibrium area fractions (θ).[3, 7, 15]

All experiments were performed on Si(001) samples with ~10^{-20} cm^{-3} B concentration, patterned with square pits (5 μm to 30 μm aside and ~90 nm deep) using reactive ion etching. After thorough rinses in acetone and ethanol, the native surface oxide was removed by a brief flash to 1250°C in UHV, using e-beam heating. The sample temperature was measured with a W-Re thermocouple, calibrated by comparison with the known temperature of the Si(111) (1x1)↔(7x7) transition, and pyrometer measurements. The estimated temperature accuracy is ~20°C, with a same-sample precision better than 5°C. Si was deposited on the surface from a collimated e-beam evaporator, containing a Si slug (99.9999 % purity). The relative flux from the evaporator was measured by an ion current monitor. The absolute flux was not measured, but rather inferred by the flux required to balance sublimation as described below. Typical deposition rates to the surfaces were of the order of one mL/several minutes. Step-free regions were created by subliming Si at ~1050°C in UHV. Step flow during sublimation terminates at the pit walls leaving atomically smooth surfaces at the pit bottoms. Pit widths larger than ~10 μm were not used, owing to vacancy island formation prior to the full expansion of the existing vacancy island.[13, 16] The high LEEM contrast ratio between surfaces separated by single atomic steps is due to the 90° degree rotation of the electron diffraction patterns of alternating Si dimer rows.[10] A slightly tilted (0,0) beam (bright field) was used for imaging.

Above 1000°C, Si sublimation results in the formation of oval vacancy islands near pit centers, where vacancy supersaturation is the highest because of diffusion limitations.[17,18] Initial stripe growth occurs as the sample temperature is lowered below ~1000°C (Fig. 1).The cooling rate was not programmed, but the temperature was dropped as quickly as possible by abruptly decreasing the heating power (to almost zero), and then abruptly increasing it a few seconds later, to a value consistent with the chosen temperature (~850°C-950°C). Below 1000°C vacancy islands nucleate rapidly throughout the pits, becoming increasingly elongated with decreasing temperature [Fig. 1(a)-(b)]. At ~920°C islands are extremely elongated and span the pits, creating a striped appearance. The process is so fast that stripes

cover most of the pit surface well before the equilibrium temperature is reached. During stripe formation, small islands grow and large islands split into smaller ones. This differs from typical island evolution during Ostwald ripening, where small islands disappear and large ones grow, but is characteristic of stress domains.[1]

Several types of defect develop in vacancy stripe arrays created in this fashion: Fork-shaped stripes [inset in Fig. 1(c)] are formed when a growing island starts, but does not complete a longitudinal split to maintain its aspect ratio. Incomplete stripes (*i*) are the result of island growth stopped by collision with adjacent islands. Protrusions at the walls (*ii*) and adatom stripes (*iii*) are perpendicular to the vacancy stripes, and are formed by adatoms diffusing from areas of supersaturation in the immediate vicinity of vacancy islands.

Having achieved a partially ordered surface consisting of both adatom and vacancy stripe features [such as in Fig. 1(c)], it is possible to remove adatom stripes by slow sublimation [Fig. 1(d)]. Sublimation, however, inevitably leads to the creation of next (i.e. one step deeper) layer vacancy stripes [inset in Fig. 1(d)], which are perpendicular to the original stripes, and nucleate and grow faster than other defects heal. (Note the multiple incomplete stripes still present in Figure 1(d) at the moment of the formation of a next-layer vacancy island.) With further sublimation next-layer stripes expand to cover most of the pit, followed by subsequent layers of perpendicular vacancy stripes *ad infinitum*, producing a highly disordered surface. Lowering the sample temperature decreases the sublimation rate, but also decelerates defect healing via surface diffusion, and does not lead to the formation of defect-free arrays. On large terraces defects are thus numerous at all temperatures, and defect-free arrays were never formed in this fashion in any of our experiments.

To counter sublimation we use Si deposition, allowing arbitrarily long healing times at the high temperatures necessary for sufficient rate of surface diffusion. Rather than being fixed, the Si deposition rate is adjusted to avoid both vacancy defects caused by sublimation, and adatom defects arising from an oversupply of Si atoms. Under these conditions, large, defect-free stripe arrays are successfully formed on a timescale of minutes (Fig. 2). Such arrays are remarkably uniform, with a well-defined

spacing (λ). For the array in Figure 2, for example, λ=115 nm ± 2 nm, determined from image cross-sections. A 2D Fourier transform for the same array peaks at λ=115 nm. Stripes exhibit small fluctuations, mostly at the endpoints, which consist of low-stiffness S_B steps.[19]

An important question is whether λ can be controlled after formation. Defect-free arrays formed successively on the same terrace at several temperatures are shown in Figure 3(a)-(d). The corresponding temperature dependence of λ in Figure 3(e) indicates considerable latitude for control. Following the arguments of Hannon et al.[9] this increase in λ above 930°C is an indication of an increasing S_A step free energy β_A. Above 1000°C, β_A increases so much that stripes evolve into oval islands in order to minimize step length, as discussed in [9]. Below ~930°C, λ becomes constant.

Several ordering mechanisms are responsible for the increase and decrease in stripe spacing following temperature changes. Longitudinal stripe splitting and new stripe nucleation and growth decrease λ. Stripe splitting [Fig. 4(a)-(b)] begins as an increase in size and frequency of the small shape fluctuations that are always present at the stripe endpoints. The larger the temperature departure from the previous equilibrium state, the larger the amplitudes of these fluctuations. Occasionally, a fluctuation becomes large enough to start freely propagating along a stripe, eventually splitting it in two. New stripes nucleate [Fig. 4(c)] in the space between existing ones (typically after a relatively large temperature change) and quickly grow to the full length of the pit [Fig. 4(d)]. Very importantly, overcoming a barrier is required in both cases: a minimum fluctuation size for stripe splitting, and critical vacancy supersaturation for stripe nucleation. This means that a minimum temperature departure is needed for their onset, and that they may be the rate-limiting step to approaching a new equilibrium state arbitrarily closely.

Figure 5 shows two mechanisms of stripe that allow λ to increase. Stripes shrink and disappear in much the opposite fashion to their appearance (Fig. 1). The disappearance of the outermost stripes is of special interest because it proceeds very smoothly with temperature change. Stripes simply grow shorter and disappear while seemingly flowing sideways. The remaining stripes rearrange in an accordion-like fashion. For this reason, the equilibrium density values in Figure 3 were obtained following this type of

ordering. Shrinking and disappearance of stripes in the middle of arrays was relatively infrequent compared to that of outermost stripes, and mainly occurred after a large temperature change.

A second mechanism of stripe density decrease consists of the merging of neighboring stripes. This process is the reverse of the stripe splitting shown in Figure 4. It involves fluctuations during which stripe ends come in close proximity to each other, and sometimes merge. It also occurs relatively infrequently compared to the sideways disappearance.

When the sample temperature is maintained at ~850ºC for a prolonged time (typically tens of minutes), stripes transform into large oval islands in a ripening process (Fig. 6). As noted by the time stamps in the images, the ripening is very slow, owing to a low rate of surface diffusion at this temperature. This return to Ostwald ripening, as well as the increase in the area to step length ratio, indicates that below 850°C the surface structure is determined by step free energy minimization, not stress interactions. This might be caused by the increase in β_A due to decrease in thermal fluctuations at low temperature.[19]

Below ~700ºC, structure changes become unobservably slow, on the timescale of days. Preserving stripe arrays such as that in Figure 2 to room temperature is easily achieved by abruptly decreasing the heating power. The ensuing temperature decrease below 700ºC occurs in several seconds, during which stripe arrays undergo no observable change.

The λ ~85 nm plateau in Figure 3(e) and stripe transformation to oval islands below 850°C deserve mention because stripes (albeit not in defect-free arrays) have previously been found to narrow below 85 nm with temperature decrease. Jones et al. reported stripe spacings as low as ~21 nm on ~400 nm long stripes[2], and Hannon et al. reported spacings below the LEEM spatial resolution.[10] The source of this difference between our and previous work could be due to the use of Si deposition to offset sublimation. While the B surface concentration and distribution have never been measured in the temperature range of interest here (850°C to 1000°C), it is reasonable to expect that they are affected by the continuous deposition of pure Si onto the surface. If differences in B concentration are responsible for the differences in observed behavior, simultaneous B and Si deposition is a possible approach to

better understanding the role of B concentration in stripe formation, as well as to growing defect-free arrays with much smaller λ.

In all our experiments, equilibrium stripe arrays entirely fill the original pit. To determine whether the area fraction of vacancy stripes (θ_v) or adatom stripes can also be controlled, and to estimate the influence of Si deposition on equilibrium stripe properties, two limiting conditions were created, shown in Figure 7. Upon excess Si deposition, vacancy stripes narrow, and adatom protrusions grow near the walls. At θ_v~0.45, adatom stripes nucleate inside the array [Fig. 4(a)]. After Si deposition is stopped, sublimation leads to stripe widening, and eventually to next-layer vacancy stripe nucleation at θ_v~0.59 [Fig. 7(b)]. Between these limits, stripe ordering is unaffected ($\lambda = 139\ \text{nm} \pm 3\ \text{nm}$ for the array in Figure 7), and appears to be an inherent property of the system, rather than a consequence of the effective Si vapor pressure created by the evaporator.

Since defect-free arrays are only stable in a narrow range around θ~½, difficulties in creating them in our and other studies are easily understood: If, owing to sublimation or for other reasons, θ is appreciably different from ½, defects will persist indefinitely, irrespective of the potential for spontaneous defect healing via surface diffusion. The observed stability for θ~½ is in agreement with stress domain theory for systems with long-ranged interactions between boundaries.[4, 7] Note that this area fraction limitation no longer holds once coarsening begins below 850°C, because the system morphology is no longer governed by stress interactions. This is seen in Figure 6(c)-(d), where a slight sublimation overcompensation (i.e. excess Si deposition) leads to a decrease in θ_v, but not to the formation of adatom islands.

In summary, we have demonstrated the creation of large (~8μm x 8μm) self-assembled defect-free stripe arrays, by using Si deposition on the atomically flat Si(001) surface with high B doping. We have identified a relationship between temperature and the stripe spacing, and determined a coverage stability range consistent with the nature of the long-ranged interactions between boundaries in the stress domain theory. Given the ability to control the stripe spacing via the preparation temperature, and to preserve the stripe arrays to room temperature, this structure may lend itself as a template for nanowire growth.

As stripe length was only limited by maximum terrace size, there is no *a priori* obstacle to growing considerably larger defect-free stripe arrays.

We thank D. Tibbetts who etched the Si samples. This work was funded by the United States Department of Energy, Office of Basic Energy Sciences, Department of Material Science and Engineering. Sandia National Laboratories is a multi-program laboratory operated by Sandia Corporation, a wholly owned subsidiary of Lockheed Martin Company, for the U.S. Department of Energy's National Nuclear Security Administration under contract DE-AC0494AL85000.

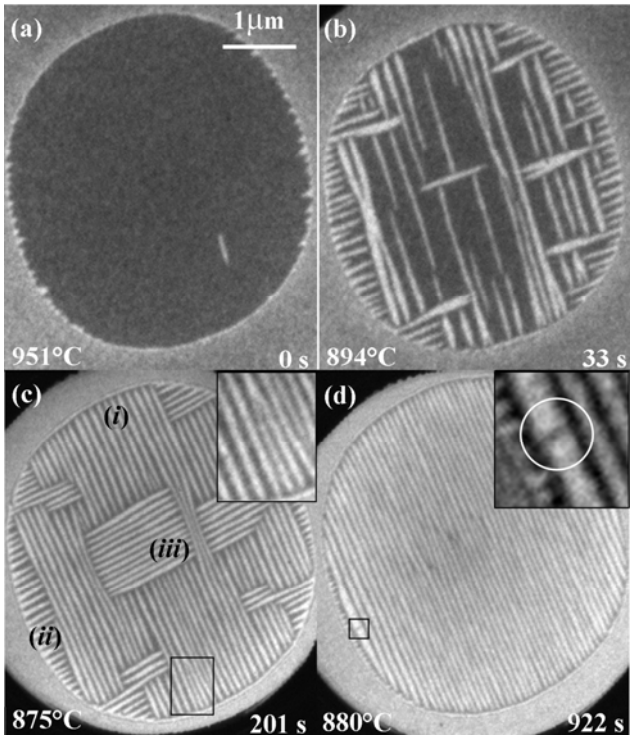

Fig. 1. LEEM image sequence of initial stripe array formation. (a) Onset of vacancy stripe formation on an atomically flat surface. The atomically smooth pit bottom is dark, and the newly formed vacancy stripe is white. (b) Stripe growth and defect formation. (c) Stripe array with several types of defects: Forked stripe (enlarged inset); (*i*) incomplete stripes; (*ii*) adatom protrusions; (*iii*) adatom stripes. (d) A partially ordered stripe array showing many incomplete stripes and a small next layer vacancy stripe (enlarged square inset).

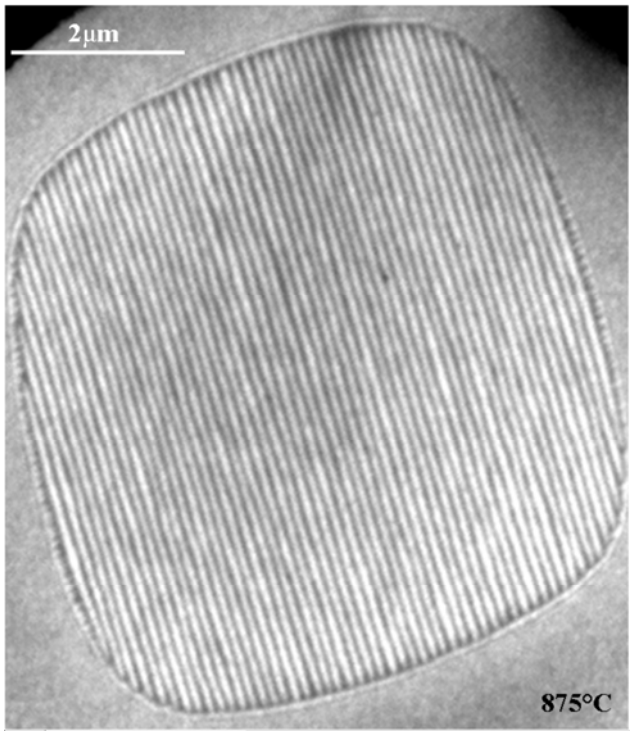

Fig. 2. LEEM image of a defect-free stripe array formed after 2 minutes at 875°C. Stripes are 6.5 μm long, ~60 nm wide, and 0.14 nm deep.

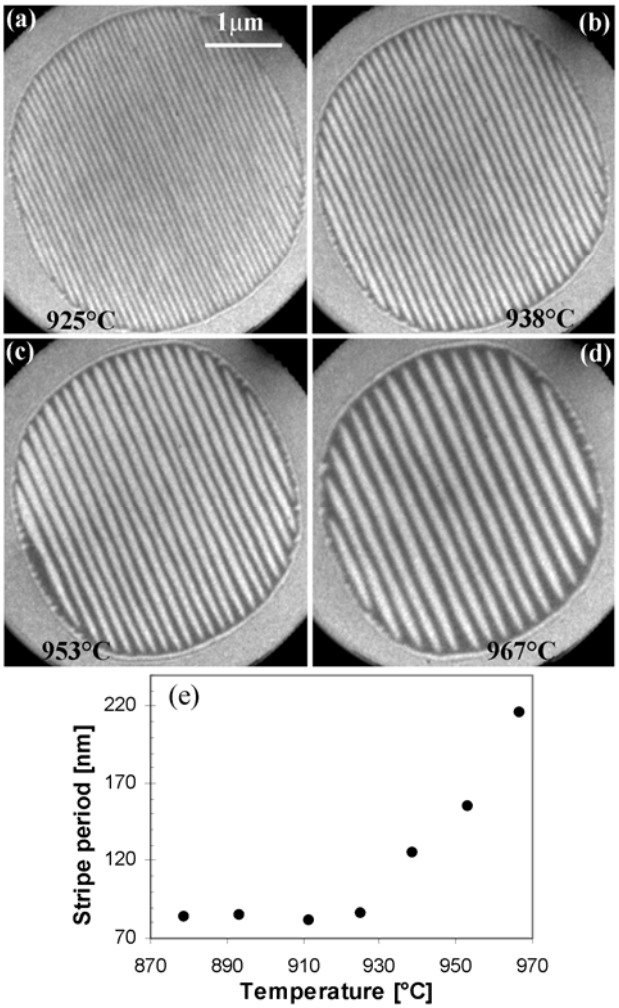

Fig. 3. LEEM images of stripe arrays formed at several temperatures in the same pit (a-d). Corresponding stripe spacing dependence on temperature (e). Below ~850°C stripes do not form, and the spacing becomes undefined.

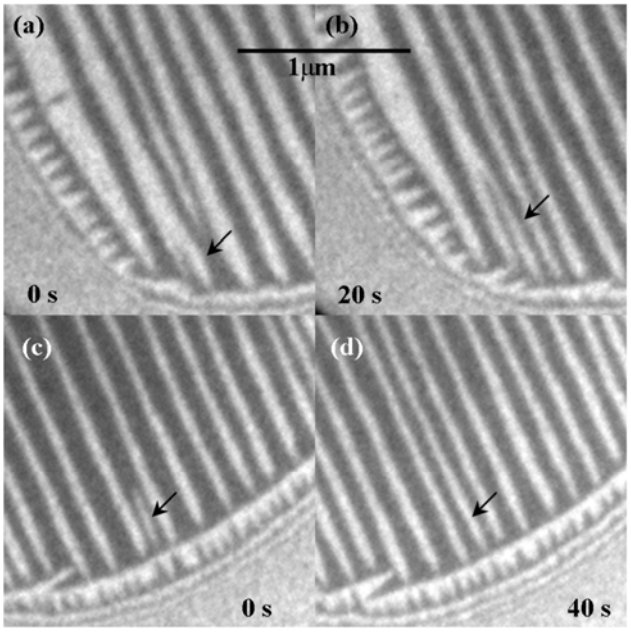

Fig. 4. LEEM images of stripe spacing decrease via longitudinal stripe splitting (a-b), and new stripe nucleation (c-d), at 905°C.

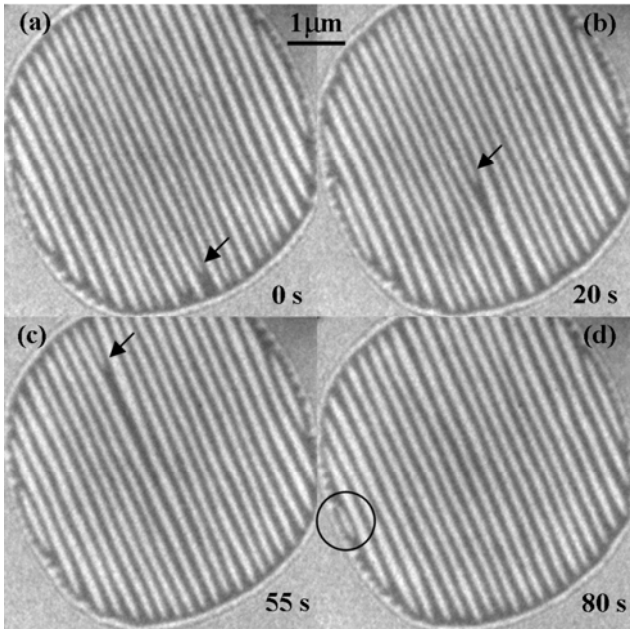

Fig. 5. LEEM image sequence of stripe spacing increase via stripe shrinking in the middle of an array (arrows), and at the periphery (circle) at 958°C.

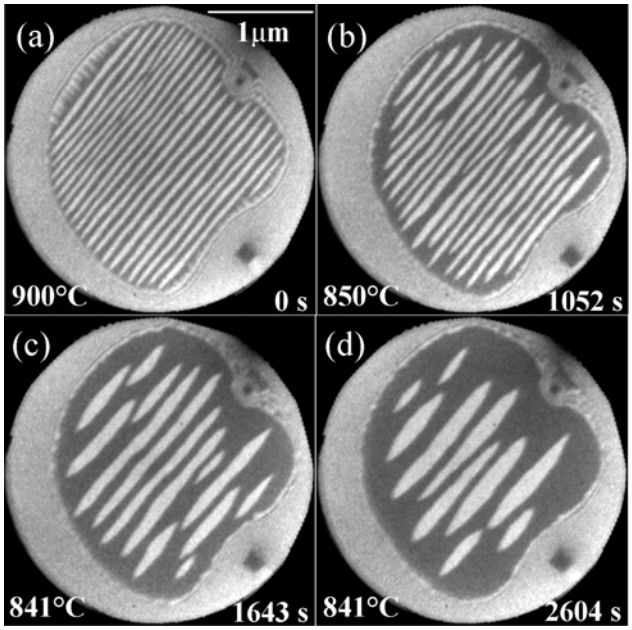

Fig. 6. LEEM image sequence of stripe coarsening.

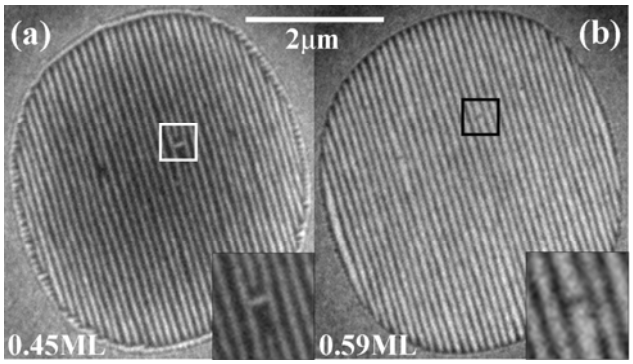

Fig. 7. LEEM images of a stripe array under two limiting conditions: (a) Si deposition leads to adatom stripe nucleation; (b) Sublimation leads to next-layer vacancy stripe nucleation.

[1] H. Ibach, Surface Science Reports **29**, 193 (1997).
[2] D. E. Jones, J. P. Pelz, Y. Hong, E. Bauer, and I. S. T. Tsong, Physical Review Letters **77**, 330 (1996).
[3] V. I. Marchenko, Journal of Theoretical and Experimental Physics **33**, 381 (1981).
[4] O. L. Alerhand, D. Vanderbilt, R. D. Meade, and J. D. Joannopulos, Physical Review Letters **61**, 1973 (1988).
[5] M. M. Hurley and S. J. Singer, Physical Review B **46**, 5783 (1992).
[6] J. Tersoff and R. M. Tromp, Physical Review Letters **70**, 2782 (1993).
[7] K.-O. Ng and D. Vanderbilt, Physical Review B **52**, 2177 (1995).
[8] A. Li, F. Liu, and M. G. Lagally, Physical Review Letters **85**, 1922 (2000).
[9] J. B. Hannon, N. C. Bartelt, B. S. Swartzentruber, J. C. Hamilton, and G. L. Kellogg, Physical Review Letters **79**, 4226 (1997).
[10] J. B. Hannon, B. S. Swartzentruber, G. L. Kellogg, and N. C. Bartelt, Surface Review and Letters **5**, 1159 (1998).
[11] J.-F. Nielsen, H.-J. Im, J. P. Pelz, M. Krueger, B. Borovsky, and E. Ganz, Journal of Vacuum Science and Technology A **17**, 1670 (1999).
[12] Z. Liu, Z. Zhang, and X. Zhu, Physical Review B **77**, 035322 (2008).
[13] S. Tanaka, C. C. Umbach, J. M. Blakely, R. M. Tromp, and M. Mankos, Applied Physics Letters **69**, 1235 (1996).
[14] J.-F. Nielsen, J. P. Pelz, H. Hibino, C.-W. Hu, I. S. T. Tsong, and J. Kouvetakis, Applied Physics Letters **79**, 3857 (2001).
[15] D. Vanderbilt, Surface science Letters **268**, L300 (1992).
[16] J.-F. Nielsen, J. P. Pelz, H. Hibino, C.-W. Hu, and I. S. T. Tsong, Physical Review Letters **87**, 136103 (2001).
[17] R. M. Tromp and M. Mankos, Physical Review Letters **81**, 1050 (1998).
[18] R. M. Tromp and J. B. Hannon, Surface Review and Letters **42**, 1565 (2002).
[19] N. C. Bartelt and R. M. Tromp, Physical Review B 54, 11731 (1996).